JCI insight

Impaired ketogenesis and increased acetyl-CoA oxidation promote hyperglycemia in human fatty liver

Justin A. Fletcher, … , Shawn C. Burgess, Jeffrey D. Browning

JCI Insight. 2019;4(11):e127737. https://doi.org/10.1172/jci.insight.127737.

Research Article | Hepatology | Metabolism

Graphical abstract

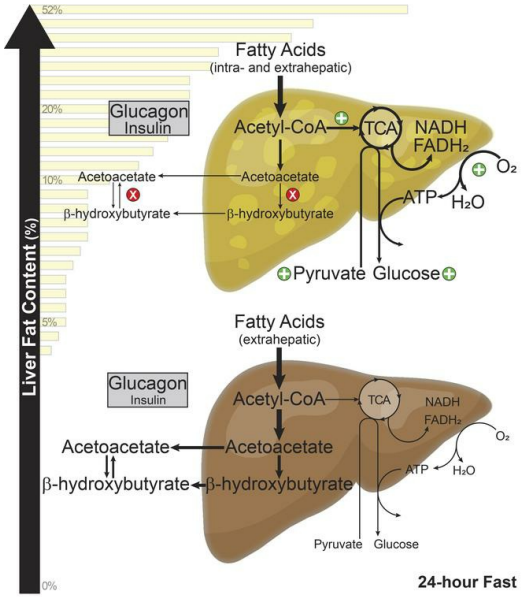

Find the latest version:

https://jci.me/127737/pdf

JCI insight

RESEARCH ARTICLE

Impaired ketogenesis and increased acetyl-CoA oxidation promote hyperglycemia in human fatty liver

Justin A. Fletcher,[1] Stanisław Deja,[1,2] Santhosh Satapati,[3,4] Xiaorong Fu,[1] Shawn C. Burgess,[1,3] and Jeffrey D. Browning[4,5,6]

[1]Center for Human Nutrition, [2]Department of Biochemistry, [3]Department of Pharmacology, [4]Advanced Imaging Research Center, [5]Department of Internal Medicine, and [6]Department of Clinical Nutrition, University of Texas Southwestern Medical Center at Dallas, Dallas, Texas, USA.

Nonalcoholic fatty liver disease (NAFLD) is a highly prevalent, and potentially morbid, disease that affects one-third of the US population. Normal liver safely accommodates lipid excess during fasting or carbohydrate restriction by increasing their oxidation to acetyl-CoA and ketones, yet lipid excess during NAFLD leads to hyperglycemia and, in some, steatohepatitis. To examine potential mechanisms, we studied flux through pathways of hepatic oxidative metabolism and gluconeogenesis using 5 simultaneous stable isotope tracers in ketotic (24-hour-fasted) individuals with a wide range of hepatic triglyceride content levels (0%–52%). Ketogenesis was progressively impaired as hepatic steatosis and glycemia worsened. Conversely, the alternative pathway for acetyl-CoA metabolism, oxidation in the tricarboxylic acid (TCA) cycle, was upregulated in NAFLD as ketone production diminished and positively correlated with rates of gluconeogenesis and plasma glucose concentrations. Increased respiration and energy generation that occurred in liver when β-oxidation and TCA cycle activity were coupled may explain these findings, inasmuch as calculated hepatic oxygen consumption was higher during fatty liver and highly correlated with gluconeogenesis. These findings demonstrate that increased glucose production and hyperglycemia in NAFLD is a consequence not of acetyl-CoA production per se, but rather of how acetyl-CoA is further metabolized in liver.

Introduction

The ectopic deposition of excess triglycerides (TGs) in liver is a known complication of obesity and insulin resistance (1). In humans, this condition is called nonalcoholic fatty liver disease (NAFLD), a term covering pathologies ranging from simple hepatic steatosis to steatohepatitis (NASH) — an inflammatory condition that can lead to chronic liver disease and cirrhosis (2). This disease is highly prevalent, with an estimated 107 million affected individuals in the United States as of 2017 (3, 4). It has been established that in the setting of insulin resistance and NAFLD, accrual of hepatic TG occurs due to increased de novo lipogenesis (DNL) (5, 6) and increased delivery of nonesterified fatty acids (NEFAs) from peripheral lipolysis (7). What remains controversial is the role of lipid disposal pathways, and more specifically β-oxidation, in the pathogenesis and progression of NAFLD. Under fasting conditions, normal human livers have the remarkable capacity to dispose of up to ≈250 g NEFAs per day by coupling β-oxidation with ketogenesis (8). A similar compensation occurs during dietary carbohydrate restriction and is associated with beneficial metabolic effects, rather than the metabolic dysfunction encountered in NAFLD (9–12). It is not clear whether this compensation fails in NAFLD or is harmful during sustained lipid availability.

Mitochondrial β-oxidation is the dominant oxidative pathway for disposal of NEFAs in liver (13). Once NEFAs enter the mitochondria via the carnitine acyltransferase system, they undergo this 4-step catabolic process, yielding reducing equivalents (NADH and flavin adenine dinucleotide [$FADH_2$]) and acetyl-CoA. Human studies have demonstrated that hepatic oxidative metabolism is increased in obesity and insulin resistance using a variety of techniques, including oxygen consumption by arterial/venous difference (14), hepatic heat production (15), positron emission tomography (16), and stable isotope tracers (7, 17). Respiration studies of isolated human liver mitochondria indicate that increased oxidative capacity is

Authorship note: JAF and SD contributed equally to this work.

Conflict of interest: The authors have declared that no conflict of interest exists.

Submitted: January 28, 2019
Accepted: April 17, 2019
Published: June 6, 2019.

Reference information: *JCI Insight*. 2019;4(11):e127737. https://doi.org/10.1172/jci.insight.127737.

an adaptive response to obesity and NAFLD, and that the loss of this response is associated with oxidative stress and the histological hallmarks of NASH (18). Ultimately, mitochondrial function, including oxidative capacity and redox defenses, is lost as NAFLD proceeds to NASH (19).

In liver, acetyl-CoA derived from β-oxidation has 2 major fates: (i) oxidation to form CO_2 in the tricarboxylic acid (TCA) cycle; or (ii) condensation in the ketogenic pathway to form acetoacetate (AcAc) or β-hydroxybutyrate (BHB). The former increases the yield of reducing equivalents from β-oxidation by ≈3-fold, and hence strongly influences respiration and ATP synthesis. In contrast, ketones cannot be oxidized in liver, but are exported and utilized by peripheral tissues, with little further impact on hepatic energetics. In humans, calorie or carbohydrate restriction substantially increases hepatic NEFA delivery and β-oxidation but attenuates acetyl-CoA oxidation in the TCA cycle, leading to ketone synthesis and the characteristic ketosis of these interventions (20, 21). Postabsorptive circulating NEFAs and hepatic β-oxidation are similarly elevated in NAFLD, but acetyl-CoA disposal is primarily linked to the TCA cycle despite no apparent defect in ketogenesis (7). Hence, NAFLD provokes increased oxidative metabolism, either because liver requires the additional respiration (22) or because ketogenesis is not sufficiently activated (23, 24).

Although the majority of the acetyl-CoA produced by normal liver (≈85%) is condensed to form ketones under ketotic conditions (25), the role and importance of the ketogenic pathway in human NAFLD pathophysiology are largely unknown. In mice, both acetyl-CoA disposal pathways are activated during the onset of obesity and hepatic steatosis, but the ketogenic response diminishes as exposure to an obesogenic diet increases (failure to suppress or augment in response to insulin or fasting, respectively) (26). Ketonemia in human NAFLD shows similar conditional variability, with 2 studies suggesting that ketone production is impaired during mildly ketotic conditions (27, 28). This may be clinically relevant, given that impaired ketogenesis in rodents is sufficient to exacerbate steatosis, stimulate the TCA cycle, increase gluconeogenesis and DNL, and promote liver injury — all characteristic features of NAFLD and NASH (23, 24). Data from overnight-fasted individuals suggest that ketogenesis is intact in those with NAFLD (7); however, a 12-hour fast does not fully activate ketogenesis or lead to ketosis in humans and may be insufficient to expose defects in this pathway. Understanding how fatty liver alters the capacity to upregulate ketone body production in humans is salient, given the increasing clinical interest in ketogenic diets, intermittent fasting, and pharmacological approaches that influence ketosis as therapies for obesity and NAFLD.

In the present study, 5 stable isotope tracers were administered simultaneously to characterize the metabolic pathways of gluconeogenesis, TCA cycle, and ketogenesis. To examine the adaptive capacity of hepatic fat oxidation and ketogenesis, ketosis was induced by a 24-hour fast in 40 individuals with a range of hepatic TG content levels (0%–52%). We report that ketogenesis, and more specifically BHB production, was progressively impaired with increasing hepatic TG content. Resistance to ketosis among NAFLD subjects was not associated with reduced rates of β-oxidation but was associated with increased acetyl-CoA oxidation in the TCA cycle, increased respiration, and elevated rates of gluconeogenesis and endogenous glucose production (EGP). Thus, during NAFLD, liver increases oxidative metabolism rather than safely disposing of excess NEFAs as ketones.

Results

Baseline characteristics of the study population. Study subjects had a range of hepatic TG contents (0%–52%, Figure 1A). Those with concentrations ≥5% (23 of 40 subjects) were considered to have NAFLD (Figure 1B). The NAFLD group was further separated into tertiles of liver fat to highlight the relationship between liver fat and other variables. Tertiles 1–3 had mean hepatic TG content of 6% ± 1%, 13% ± 2%, and 30% ± 4%, respectively. Age, sex distribution, and ethnic/racial makeup were similar among the groups (Table 1). As anticipated, there was a greater proportion of obese subjects with impaired insulin sensitivity and hyperlipidemia among those with NAFLD. Serum aspartate aminotransferase (AST) was slightly higher among those with fatty liver, while serum alanine aminotransferase (ALT) was ≈2-fold higher. Neither group had laboratory evidence of hepatic synthetic dysfunction or portal hypertension. As anticipated, subjects with NAFLD had impaired glucose disposal during hyperinsulinemic-euglycemic (H-E) clamp (Figure 1C). However, peripheral insulin sensitivity was similar across the different levels of hepatic TG content in the NAFLD group.

Insulin resistance was associated with an impaired metabolic transition to the fasted state in NAFLD subjects. We next examined the metabolic and biochemical response of the subjects to a 12- and 24-hour fast. Indirect calorimetry demonstrated that respiratory quotients (RQs) were similar between the 2 groups and changed physiologically over the course of the study in a manner consistent with fasting (Figure 1D).

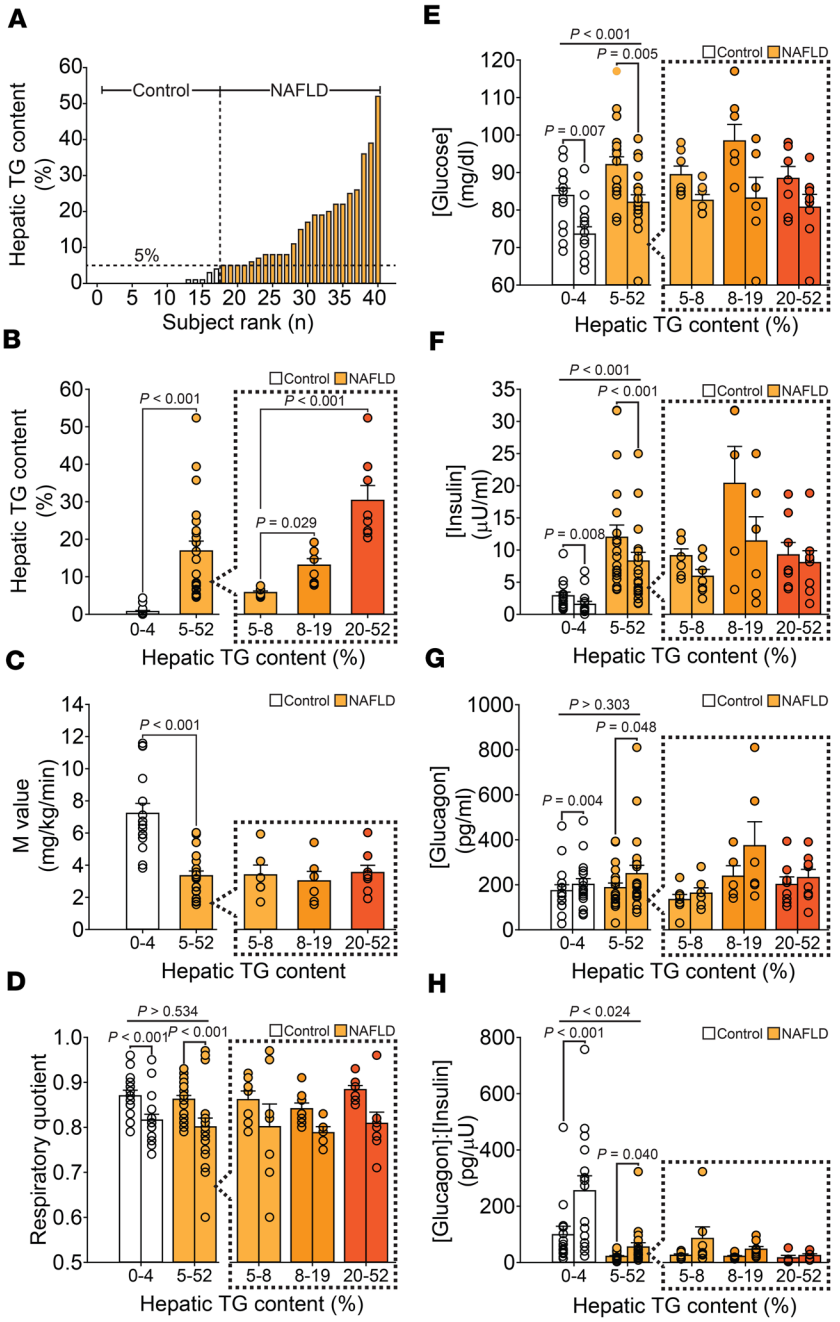

Figure 1. Hepatic TG content, insulin sensitivity, and biochemical response to a 24-hour fast. (**A**) Hepatic TG content was measured by ^{1}H-MRS and is shown by rank (range: 0%–52%; n = 40). (**B**) Using a hepatic TG cutoff of 5%, the population was dichotomized into control (n = 17) and NAFLD (n = 24) groups. The NAFLD group was further separated into tertiles of liver fat, with tertiles 1–3 having mean hepatic TG content of 6% ± 1% (n = 7), 13% ± 2% (n = 8), and 30% ± 4% (n = 8), respectively ($P < 0.004$). (**C**) Mean glucose disposal rates (M value) during H-E clamp were significantly lower in the NAFLD group (n = 20), consistent with insulin resistance. (**D**) Respiratory quotients were similar in control (n = 15) and NAFLD (n = 20) subjects and declined from 12 (left bars) to 24 hours (right bars) of fasting, consistent with fasting physiology. (**E**) Plasma glucose concentrations at 12 and 24 hours of fasting were higher in NAFLD subjects (n = 22) compared with controls (n = 16) and declined in both groups as the fasting duration increased. (**F**) Plasma insulin and (**G**) glucagon concentrations as well as (**H**) glucagon/insulin ratio at 12 and 24 hours of fasting are shown for control (n = 15) and NAFLD (n = 19) subjects. Fasting changes in concentrations of plasma insulin and glucagon, as well as the glucagon/insulin ratio, were observed in both groups; however, insulin was consistently higher, and glucagon/insulin ratio lower, among NAFLD subjects. Plasma concentrations of glucose, insulin, and glucagon were similar among the tertiles of liver fat. Significance was determined using 2-tailed Student's t test for paired and unpaired data and 1-way ANOVA and 2-way repeated-measures ANOVA when appropriate.

Plasma glucose concentrations were higher in NAFLD subjects at all points in the study and declined in both groups as the fasting duration increased (Figure 1E). Fasting also induced the expected changes in concentrations of plasma insulin (decreased) and glucagon (increased), as well as glucagon/insulin ratios (increased) in both groups (Figure 1, F–H); however, insulin concentrations were consistently higher and glucagon/insulin ratios lower among NAFLD subjects. Plasma concentrations of glucose, insulin, and glucagon were similar among the tertiles of hepatic steatosis.

The metabolic response of plasma NEFAs and ketones were blunted at the extremes of plasma insulin concentrations in NAFLD subjects. Changes in plasma NEFA and ketone concentrations differed significantly between control and NAFLD subjects in response to fasting (Figure 2, A and B). To control for insulin action, we examined plasma NEFA and ketone concentrations during an H-E clamp and found that both were higher (≈98% and ≈30%, respectively) among those with fatty liver. However, in 12-hour-fasted subjects (without H-E clamp), plasma ketones were normal in those with NAFLD despite circulating NEFAs that

Table 1. Characteristics of control and NAFLD subjects

	Group		
	Control (n = 17)	NAFLD (n = 23)	P value
Age (yr)	39 ± 3	45 ± 3	0.172
Sex (F/M)	10:7	15:8	0.934
Ethnicity/race, n (%)			
Hispanic	2 (12.5)	8 (33.3)	0.145
Non-Hispanic Black	7 (43.8)	3 (12.5)	0.066
Non-Hispanic White	8 (43.8)	10 (45.8)	0.923
Asian	0 (0.0)	1 (4.2)	1.000
American Indian	0 (0.0)	1 (4.2)	1.000
BMI (kg/m^2)	26 ± 1	32 ± 1	<0.001
Body fat (%)	32 ± 2	38 ± 2	0.029
Lean mass (kg)	50 ± 2	54 ± 3	0.247
Fasting glucose (mg/dl)	87 ± 1	102 ± 4	0.001
Fasting insulin (μU/ml)	5.8 ± 2.9	14.8 ± 3.4	<0.001
Hemoglobin A1c (%)	5.4 ± 0.1	5.9 ± 0.2	0.028
Total cholesterol (mg/dl)	179 ± 11	210 ± 10	0.043
HDL-c (mg/dl)	59 ± 3	48 ± 3	0.022
LDL-c (mg/dl)	102 ± 11	125 ± 8	0.111
TGs (mg/dl)	90 ± 14	183 ± 19	<0.001
AST (U/l)	24 ± 3	35 ± 6	0.035
ALT (U/l)	25 ± 4	52 ± 11	0.035
Albumin (mg/dl)	4.4 ± 0.1	4.6 ± 0.1	0.420
Platelet count (×1000)	237 ± 13	245 ± 11	0.635

Values are mean ± SEM unless otherwise stated. Data analyzed by Student's t test, χ^2 test, and Fisher's exact test. HDL-c, HDL cholesterol; TG, triglyceride; AST, aspartate aminotransferase; ALT, alanine aminotransferase. Conversions: glucose (mg/dl) × 0.05551 = mmol/l; insulin (μU/ml) × 7.175 = pmol/l; total cholesterol, HDL-c, and LDL-c (mg/dl) × 0.02586 = mmol/l; TGs (mg/dl) × 0.01129 = mmol/l; NEFA (mEq/l) × 1 = mmol/l; glucagon (pg/ml) × 1 = ng/l.

were increased by ≈29%. Together, these data are consistent with the well-known increase in basal lipolysis present in overnight-fasted NAFLD subjects (7). However, after a 24-hour fast, plasma NEFA and ketone concentrations were ≈30% lower in NAFLD subjects compared with controls. The lower plasma ketone concentrations among those with NAFLD at 24 hours of fasting were due to reduced plasma BHB, but not AcAc (Figure 2C). In fact, there was a significant inverse relationship between plasma BHB concentrations and hepatic TG content within the 24-hour fasted study population (Spearman's correlation coefficient [r_S] = –0.343, P = 0.043), indicating a relationship between steatosis severity and ketonemia. Despite these differences, plasma NEFA and ketone concentrations remained highly correlated in both groups at 24 hours of fasting (control: r_S = 0.906, P < 0.001; NAFLD: r_S = 0.821, P < 0.001).

Ketogenesis was attenuated in NAFLD subjects after a 24-hour fast. To further examine the differences noted in plasma ketone concentrations after a 24-hour fast, we measured ketogenesis via the intravenous infusion of both [3,4-$^{13}C_2$]AcAc and [1,2-$^{13}C_2$]BHB. The metabolic pathways probed in this study are summarized in Figure 3A. Unlike in overnight-fasted subjects (7), rates of ketogenesis were lower among those with NAFLD after a 24-hour fast, especially those with greater concentrations of hepatic TG (Figure 3B). The aggregate flux data were remarkably similar to plasma ketone concentrations after a 24-hour fast (Figure 2, A and C). As with plasma BHB concentrations, there was a significant inverse relationship between hepatic TG content and ketogenesis within the entire study population (r_S = –0.328, P = 0.042; Supplemental Figure 2A; supplemental material available online with this article; https://doi.org/10.1172/jci.insight.127737DS1). The lower rates of ketogenesis in NAFLD subjects were due primarily to significantly lower rates of BHB production (Figure 3D). It should be noted, however, that rates of BHB production in the present study were ≈2.9-fold higher among controls and ≈2.7-fold higher among NAFLD subjects when compared with 12-hour-fasted subjects (7), indicating that fatty liver blunts, but does not preclude, a ketogenic response to fasting. In addition, plasma ketone concentrations were correlated with ketone turnover (r_S = 0.527, P = 0.001), suggesting that

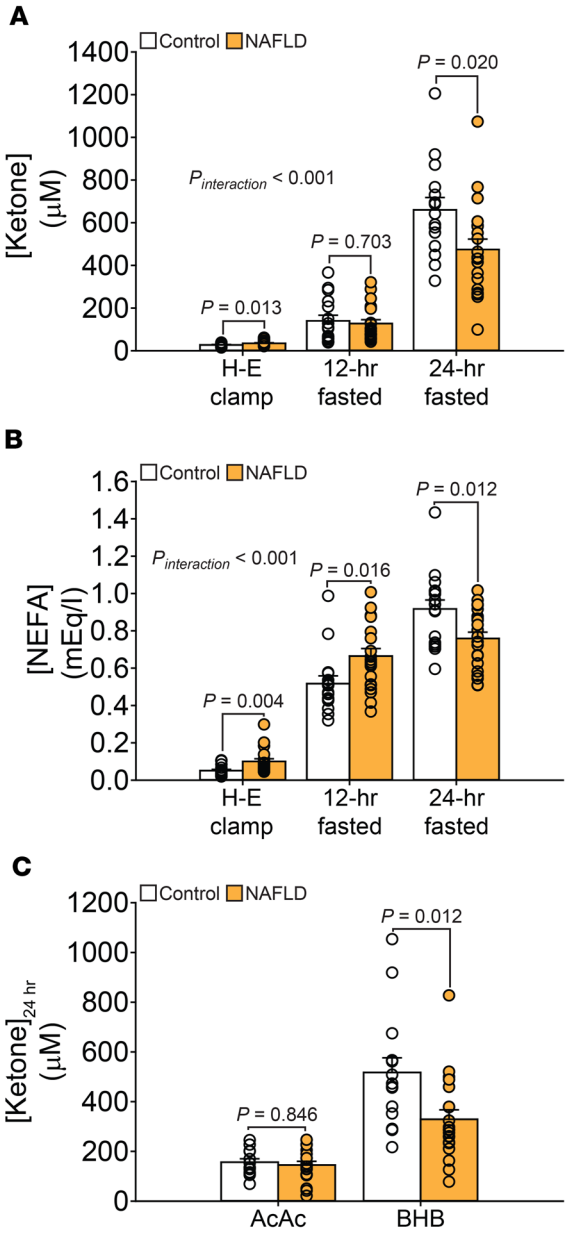

Figure 2. Fasting ketosis is impaired in subjects with NAFLD. Plasma (**A**) ketones and (**B**) NEFAs were measured during H-E clamp and after a 12- and 24-hour fast. Both ketone (control: $n = 16$, NAFLD: $n = 21$) and NEFA (control: $n = 17$, NAFLD: $n = 22$) concentrations were higher among those with fatty liver during an H-E clamp. In 12-hour-fasted subjects, plasma ketones were normal in those with NAFLD despite increased circulating NEFAs. After a 24-hour fast, plasma NEFA and ketone concentrations were ≈30% lower in NAFLD subjects compared with controls. There was a significant interaction term for both plasma ketones and NEFAs, indicating that control and NAFLD subjects respond differently to the transition from high to low insulin concentrations. (**C**) The lower plasma ketone concentrations among those with NAFLD at 24 hours of fasting were due to reduced plasma BHB, but not AcAc, concentrations. Significance was determined using 2-tailed Student's *t* test for unpaired data and 2-way repeated-measures ANOVA when appropriate.

they were reflective of ketone production rates in 24-hour-fasted humans.

Fatty liver impaired the interconversion AcAc ≒ BHB but not ketone body disposal. Given the significantly lower plasma concentrations and production rates of BHB (Figure 2, A and D), we examined the capacity for ketone body interconversion via the enzyme BHB dehydrogenase. Among those with NAFLD, regardless of hepatic TG content, the ability to convert AcAc to BHB and vice versa was significantly reduced (Figure 3, E and F). This, in conjunction with the increased plasma [AcAc]/[BHB] ratio (0.34 ± 0.04 vs. 0.48 ± 0.05, $P = 0.044$; Figure 2C), suggested that either hepatic mitochondrial redox state was more reduced in subjects with NAFLD or that BHB dehydrogenase function was impaired.

Since plasma concentrations of ketones represent the difference between utilization and production rates, we also examined rates of AcAc and BHB disposal. When compared in aggregate, there was no difference in ketone body disposal rates between control and NAFLD subjects (Figure 3, G and H); however, AcAc disposal rates tended to be lower in those with fatty liver.

Ketogenesis did not correlate with EGP or gluconeogenesis. Ketogenesis is closely related to hepatic acetyl-CoA availability. A recent report suggested that ketogenesis is a surrogate marker for hepatic acetyl-CoA content and that both measures correlate strongly with hepatic glucose production when the majority of glucose is derived from pyruvate carboxylase (i.e., gluconeogenesis) (29). To examine this relationship in humans, we assessed hepatic glucose metabolism using the intravenous infusion of [3,4-$^{13}C_2$]glucose and oral ingestion of [^{2}H]water in 24-hour-fasted subjects. The incorporation of ^{2}H into glucose H6 confirmed that the majority of glucose originated from pyruvate carboxylase in control and NAFLD subjects after 24 hours of fasting (Figure 4A and Supplemental Figure 1). Glycerol accounted for a minority of the glucose produced, while one-quarter was derived from glycogenolysis. EGP was measured by tracer dilution and found to be significantly higher in NAFLD subjects (Figure 4B). Ketogenesis tended to have an inverse correlation with EGP

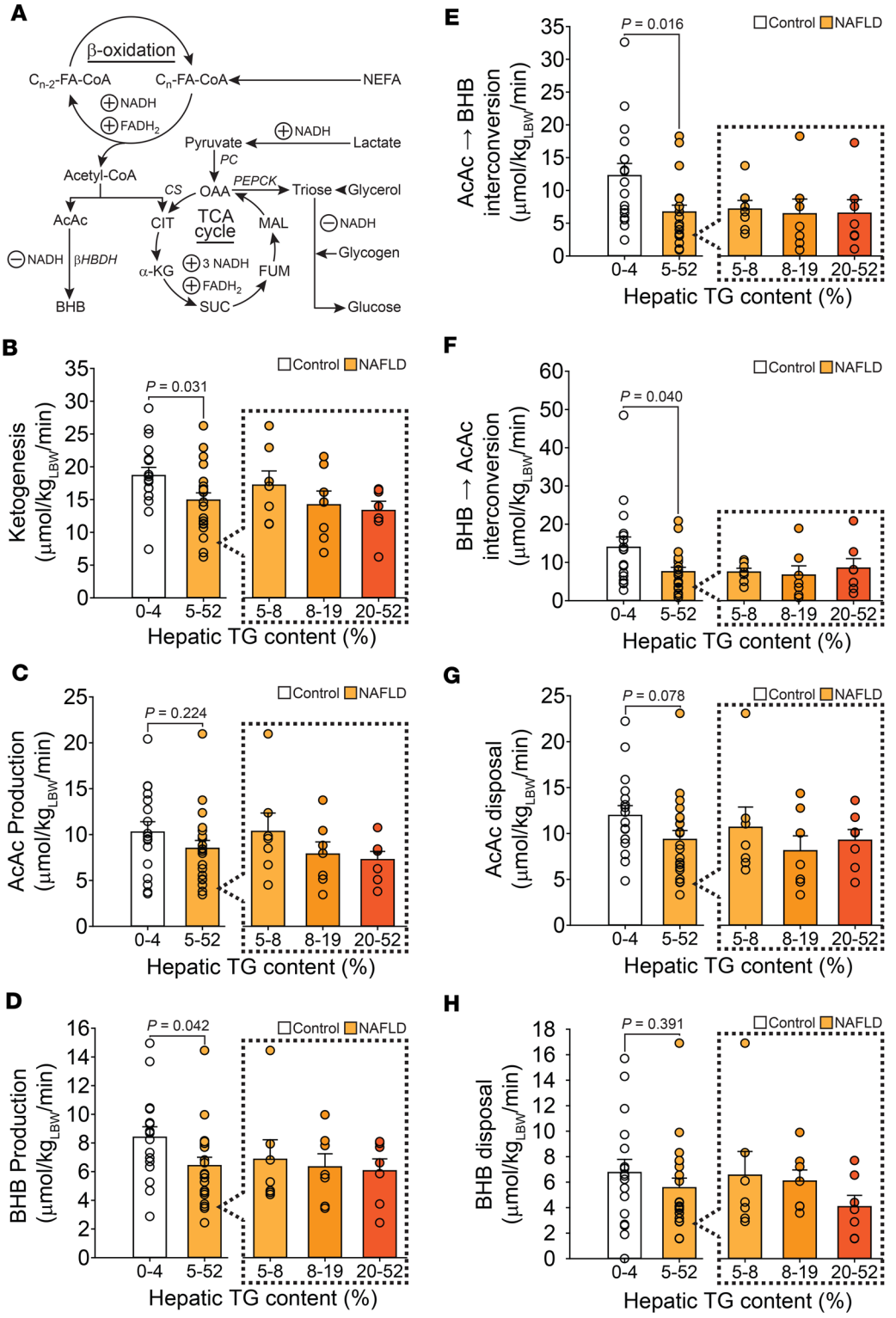
A
β-oxidation
C_{n-2}-FA-CoA
C_n-FA-CoA
NEFA
NADH
$FADH_2$
Pyruvate
Lactate
PC
Acetyl-CoA
CS
OAA
PEPCK
Triose
Glycerol
AcAc
CIT
TCA cycle
MAL
Glycogen
βHBDH
BHB
α-KG
3 NADH
FUM
SUC
Glucose
B
Ketogenesis (μmol/kg$_{LBW}$/min)
P = 0.031
Control
NAFLD
0-4
5-52
5-8
8-19
20-52
Hepatic TG content (%)
C
AcAc Production (μmol/kg$_{LBW}$/min)
P = 0.224
D
BHB Production (μmol/kg$_{LBW}$/min)
P = 0.042
E
AcAc → BHB interconversion (μmol/kg$_{LBW}$/min)
P = 0.016
F
BHB → AcAc interconversion (μmol/kg$_{LBW}$/min)
P = 0.040
G
AcAc disposal (μmol/kg$_{LBW}$/min)
P = 0.078
H
BHB disposal (μmol/kg$_{LBW}$/min)
P = 0.391

Figure 3. Ketone body production, interconversion, and disposal is impaired in NAFLD. (**A**) The pathways measured by the simultaneous administration of 5 stable isotope tracers are presented. Ketone tracers allow for the measurement of ketogenesis. The glucose and heavy water tracers allow for the sources of glucose, as well as EGP, to be determined. The propionate tracer allows for evaluation of pathways centered on the TCA cycle. Data from these tracer studies are combined to estimate hepatic β-oxidation (acetyl-CoA production) and oxygen consumption. FA-CoA, fatty acyl-CoA; NEFA, nonesterified fatty acids; PC, pyruvate carboxylase; OAA, oxaloacetate; CS, citrate synthase; PEPCK, phosphoenolpyruvate carboxykinase; AcAc, acetoacetate; CIT, citrate; MAL, malate; FUM, fumarate; α-KG, α-ketoglutarate; BHB, β-hydroxybutyrate; SUC, succinate. (**B**) An intravenous infusion of [3,4-$^{13}C_2$]AcAc and [1,2-$^{13}C_2$]BHB combined with a 2-pool model was used to measure the rate of production of these ketones (control: n = 17, NAFLD: n = 21). Rates of ketogenesis were significantly lower among those with NAFLD and inversely correlated with hepatic TG content. LBW, lean body weight. (**C**) Rates of AcAc production did not differ between control and NAFLD subjects, but tended be lower among NAFLD subjects with higher concentrations of hepatic TG. (**D**) Rates of BHB production were lower among NAFLD subjects, especially those with higher hepatic TG concentrations. (**E**) Rates of interconversion of AcAc ⇌ BHB and (**F**) BHB ⇌ AcAc were lower among NAFLD subjects. (**G**) Disposal rates for AcAc tended to be lower in all NAFLD subjects and was significantly lower among those with higher concentrations of hepatic TG. (**H**) Rates of BHB disposal were similar between control and NAFLD subjects in aggregate, but tended to be lower among those the highest hepatic TG concentrations. Ketone isotopic data was unavailable for 2 NAFLD subjects. Significance was determined using 2-tailed Student's t test for unpaired data and 1-way ANOVA when appropriate.

(r_S = –0.297, P = 0.074). We therefore combined the ^{2}H and ^{13}C tracer data to determine absolute rates of glucose production from pyruvate carboxylase. There was no significant relationship between ketogenesis and gluconeogenesis (r_S = 0.014, P = 0.936; Supplemental Figure 2B) or plasma glucose concentrations (r_S = –0.270, P = 0.110; Supplemental Figure 2C). Rates of gluconeogenesis were also significantly higher among subjects with NAFLD despite lower rates of ketogenesis (Figure 4B). In addition, there was no discernable relationship between BHB production rates alone and EGP or gluconeogenesis in the present study, or when data from 12-hour-fasted control and NAFLD subjects studied previously were reexamined (7). Thus, the rate of ketogenesis was not specifically associated with the control of gluconeogenesis in humans.

Impaired ketogenesis was associated with increased acetyl-CoA disposal in the TCA cycle. If the majority of acetyl-CoA produced in liver is condensed to form ketones, then rates of ketogenesis should reflect hepatic acetyl-CoA production and, by corollary, content (29). We therefore examined the alternative disposal pathway for acetyl-CoA — oxidation in the TCA cycle — by combining ^{2}H and ^{13}C isotopomer analysis of glucose following oral ingestion of [U-$^{13}C_3$]propionate with a quantitative model of hepatic metabolism. Pyruvate carboxylase represents one of the most significant anaplerotic pathways of the TCA cycle and acts as a control point for gluconeogenesis by regulating the conversion of pyruvate to oxaloacetate (Figure 3A). Tracer data indicated that anaplerosis was markedly increased in those with NAFLD despite their lower rates of ketogenesis and, presumably, hepatic acetyl-CoA content — the allosteric activator of pyruvate carboxylase (Figure 4C). In contrast to ketogenesis, the oxidation of acetyl-CoA in the hepatic TCA cycle was ≈57% higher among NAFLD subjects (Figure 4D). Unlike ketogenesis, TCA cycle activity was positively correlated with hepatic TG content levels (r_S = 0.431, P = 0.007; Supplemental Figure 3C), rates of gluconeogenesis (r_S = 0.460, P = 0.003; Supplemental Figure 3D), and plasma glucose concentrations (r_S = 0.602, P < 0.001; Supplemental Figure 3E). It is notable that, compared with 12-hour-fasted subjects (7), TCA cycle activity was reduced after fasting for 24 hours by ≈60% and ≈50% in control and NAFLD subjects, respectively, again indicating a preserved but blunted metabolic response to fasting in those with fatty liver.

Altered acetyl-CoA disposal in NAFLD was associated with increased plasma pyruvate concentrations. Increased oxidation of acetyl-CoA in the TCA cycle, and reduced condensation to ketones, may be related to the availability of oxaloacetate or its precursors (see Figure 3A) (30). We examined plasma concentrations of lactate and pyruvate in a subset of subjects from both groups during the transition from fed to fasting. Plasma lactate concentrations did not differ between the groups at any time point during the study. Plasma pyruvate concentrations were similar between the 2 groups during H-E clamp and declined in both groups as the fasting duration increased (Figure 4E). However, NAFLD subjects had, or tended to have, higher pyruvate concentrations at 12 and 24 hours of fasting, respectively. This is consistent with reduced peripheral pyruvate oxidation (31) and increased Cori cycling during insulin resistance. Elevated pyruvate and increased rates of pyruvate carboxylase flux in NAFLD may not only increase gluconeogenesis, but also raise hepatic oxaloacetate concentrations, which would activate TCA cycle oxidation and reduce the rate of ketogenesis.

The rate of hepatic acetyl-CoA production is normal but its metabolic fate is altered in NAFLD subjects. Acetyl-CoA production (β-oxidation) was estimated by combining rates of ketogenesis and TCA cycle turnover (see Figure 3A). Despite the differences in EGP and gluconeogenesis between control and NAFLD subjects, rates of β-oxidation did not differ (Figure 4F). In addition, there was no significant relationship between estimated β-oxidation and EGP (r_S = –0.168, P = 0.325) or gluconeogenesis (r_S = 0.077, P = 0.652; Supplemental Figure 4A). Of the acetyl-CoA produced in control subjects, 86% ± 2% was used for ketogenesis, a value in agreement with

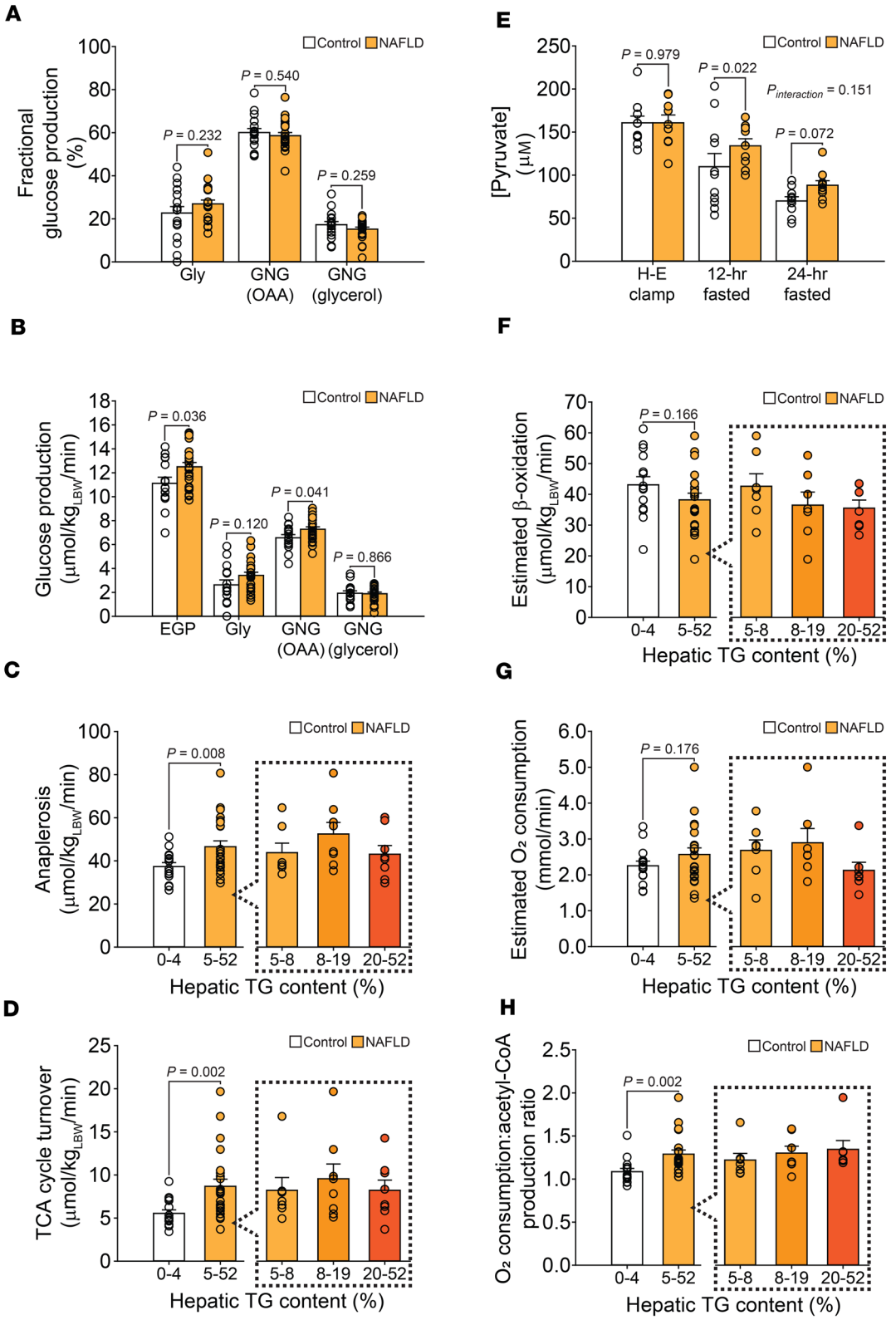
A
Fractional glucose production (%)
Control NAFLD
P = 0.232
P = 0.540
P = 0.259
Gly
GNG (OAA)
GNG (glycerol)
B
Glucose production (μmol/kgLBW/min)
P = 0.036
P = 0.120
P = 0.041
P = 0.866
EGP
Gly
GNG (OAA)
GNG (glycerol)
C
Anaplerosis (μmol/kgLBW/min)
P = 0.008
0-4
5-52
5-8
8-19
20-52
Hepatic TG content (%)
D
TCA cycle turnover (μmol/kgLBW/min)
P = 0.002
E
[Pyruvate] (μM)
P = 0.979
P = 0.022
Pinteraction = 0.151
P = 0.072
H-E clamp
12-hr fasted
24-hr fasted
F
Estimated β-oxidation (μmol/kgLBW/min)
P = 0.166
G
Estimated O2 consumption (mmol/min)
P = 0.176
H
O2 consumption:acetyl-CoA production ratio
P = 0.002

Figure 4. Increased hepatic glucose production in NAFLD is associated with increased acetyl-CoA oxidation and oxygen consumption. (**A**) Fractional glucose production was determined using the ^2H_2O method. Fractional glycogenolysis (Gly) and gluconeogenesis (GNG) were similar in control (n = 17) and NAFLD (n = 23) subjects at 24-hours of fasting. (**B**) Infusion of [3,4-$^{13}C_2$]glucose was used to determine EGP. Absolute rates of glycogenolysis, as well as gluconeogenesis from OAA and glycerol, were determined by combining EGP with fractional glucose production data. There was a higher rate of EGP in NAFLD subjects due to an increased rate of gluconeogenesis from OAA. (**C**) Carbon-13 isotopomer analysis of plasma glucose indicated that total anaplerosis was significantly higher in NAFLD (n = 23) compared with control (n = 15) subjects. (**D**) TCA cycle turnover was increased among NAFLD subjects compared with controls. (**E**) Oxaloacetate and its precursors, such as pyruvate, can stimulate TCA cycle activity. Plasma pyruvate concentrations were similar in the 2 groups during H-E clamp and declined in both groups as the fasting duration increased; however, NAFLD subjects had, or tended to have, higher pyruvate concentrations at 12 and 24 hours of fasting, respectively (control: n = 11, NAFLD: n = 9). (**F**) Estimated β-oxidation did not differ between the groups in aggregate, but tended to be lower among those with higher concentrations of hepatic TG (control: n =15, NAFLD: n = 21). (**G**) In aggregate, NAFLD subjects had O_2 consumption rates that were similar to those of controls. This was due to a variable effect of hepatic TG content, as those with mild to moderate hepatic steatosis tended to have higher $\dot{V}O_2$ than controls. (**H**) NAFLD subjects consumed ≈30% more O_2 for each acetyl-CoA produced. Glucose isotopic data was unavailable for 2 control subjects. Combined isotopic data were unavailable for 2 control and 2 NAFLD subjects. Significance was determined using 2-tailed Student's t test for unpaired data, 1-way ANOVA, and 2-way repeated-measures ANOVA when appropriate.

normal fasting physiology (25). Ketogenesis accounted for significantly less acetyl-CoA disposal in NAFLD subjects (77% ± 2%, P = 0.003). Thus, ketogenesis is a substantial component of β-oxidation after a 24-hour fast but nevertheless a partial measure of acetyl-CoA production, which is skewed by NAFLD. Specifically, hepatic acetyl-CoA was shifted away from ketogenesis and toward oxidation in the TCA cycle in obese NAFLD subjects, but the total rate of acetyl-CoA production was not affected.

Reduced ketogenesis in NAFLD subjects leads to increased hepatic O_2 consumption. Due to the ≈3-fold increase in reducing equivalent production when β-oxidation is coupled with the TCA cycle (see Figure 3A), we examined hepatic O_2 consumption ($\dot{V}O_2$), estimated from the net production of NADH/$FADH_2$ in a flux balance analysis of β-oxidation, ketogenesis, the TCA cycle, and gluconeogenesis. When examined in aggregate, NAFLD subjects had estimated O_2 consumption rates that were similar to those of controls (Figure 4G). However, this appeared to be due to a variable effect of hepatic TG content, with the 5%–19% TG tertiles tending to be elevated and the 20%–52% tertile tending to be lower. These data are reminiscent of the temporal changes in hepatic oxidative metabolism that occur during longitudinal dietary lipid exposure in a rodent model, and isolated liver mitochondria from humans, with increasing severity of NAFLD (18, 26). Due to a ≈10% greater disposal of acetyl-CoA in the TCA cycle, NAFLD subjects consumed ≈30% more O_2 for each acetyl-CoA produced (Figure 4H). Unlike rates of ketogenesis and β-oxidation, estimated hepatic $\dot{V}O_2$ was highly correlated with both EGP (r_S = 0.574, P < 0.001) and gluconeogenesis (r_S = 0.680, P < 0.001; Supplemental Figure 4B).

Adiposity does not explain the metabolic differences between control and NAFLD subjects. To control for differences in body mass between the groups, we matched individuals from the control group with those from the NAFLD group by BMI (Supplemental Table 1). These 2 subgroups of 12 subjects had a similar BMI (27 ± 1 vs. 29 ± 1 kg/m^2, P = 0.125) and percent body fat (32% ± 3% vs. 35% ± 2%, P = 0.404), with markedly different hepatic TG content (1% ± 0% vs. 18% ± 4%, P = 0.002) and peripheral insulin sensitivity (P < 0.001). The observed differences in hepatic metabolism between the 2 groups persisted despite controlling for differences in body mass. In fact, differences between the control and NAFLD groups regarding production of AcAc (10.9 ± 1.4 vs. 7.4 ± 0.8 μmol/kg lean body weight [kg_{LBW}]/min, P = 0.045), BHB (9.2 ± 0.9 vs. 5.7 ± 1.0 μmol/kg_{LBW}/min, P = 0.017), and ketogenesis (20.1 ± 1.3 vs. 13.1 ± 1.5 μmol/kg_{LBW}/min, P = 0.002) were even more striking between obesity-matched groups.

Discussion

Ketogenesis represents an important adaptive mechanism in human physiology that allows liver to utilize stored TG to provide metabolic fuel for peripheral tissues during periods of carbohydrate deprivation. This metabolic pathway is also harnessed by liver during the early stages of an obesogenic diet (26), likely as a mechanism to safely manage excess TG-derived acetyl-CoA via nonoxidative disposal and thereby limit oxidative stress (22). In this study, we examined the effect of hepatic steatosis (range: 0%–52%, Figure 1A) on the adaptive capacity of liver to upregulate ketogenesis during the induction of ketosis by a 24-hour fast. Subjects with NAFLD exhibited a resistance to ketosis/ketonemia that manifested as reduced plasma concentrations of BHB that was related to both insulin insensitivity and severity of hepatic steatosis. Stable isotope tracer data indicated that the blunted response of plasma ketones in NAFLD subjects after a 24-hour fast was due to a progressive reduction in the ability to synthesize ketones, especially BHB, as hepatic steatosis increased. Attenuated ketogenesis in subjects with fatty liver led to a reciprocal increase

in oxidative disposal of acetyl-CoA in the TCA cycle. As a result, the rate of acetyl-CoA production (β-oxidation) was estimated to be similar between control and NAFLD subjects despite dramatic differences in the metabolic fate of acetyl-CoA. The differential utilization of acetyl-CoA in the TCA cycle in NAFLD subjects was associated with elevated rates of pyruvate carboxylase flux, gluconeogenesis, EGP, and oxygen consumption. Lower rates of ketogenesis implied decreased acetyl-CoA concentrations (29), which was in conflict with the canonical allosteric role of this molecule in the excessive stimulation of pyruvate carboxylase–mediated gluconeogenesis and EGP (Supplemental Figure 2B). In fact, the strongest predictor of gluconeogenesis among 24-hour-fasted subjects was estimated hepatic $\dot{V}O_2$, followed by pyruvate carboxylase flux and acetyl-CoA oxidation in the TCA cycle, respectively (Supplemental Figure 4B, Supplemental 3B, and Supplemental 3D). Thus, an important metabolic pathology of NAFLD is that it limits the disposal of lipids via ketogenesis, thereby favoring oxidative metabolism, which loads hepatocellular respiration, increases gluconeogenesis and EGP, and promotes elevated plasma glucose concentrations.

During fasting or carbohydrate restriction, a rise in the plasma glucagon/insulin ratio activates lipolysis and NEFA release from adipose tissue. The resulting rise in plasma NEFA concentrations contributes to increased hepatic β-oxidation and ketogenesis during these states (32). Rates of lipolysis and NEFA concentrations are similarly elevated in overnight-fasted (12 hour-fasted) subjects with NAFLD (7, 33, 34), which led us to speculate that increased NEFA delivery to liver causes the observed increase in fatty acid oxidation in these individuals (7). However, after a 24-hour fast the lipolytic response was paradoxically impaired in NAFLD subjects (Figure 2B). Similar observations have been made in obese subjects during prolonged fasting (35, 36), and the impairment may be due to relative hyperinsulinemia or, more importantly, a lower glucagon/insulin ratio (Figure 1H). Given that a 13% lower rate of ketogenesis (Figure 3B) was coincident with 16% lower plasma NEFA concentrations (Figure 2B), it is tempting to assign the mechanism of impaired fasting ketogenesis to lower circulating NEFAs in NAFLD subjects. However, the calculated rate of β-oxidation was similar in 24-hour-fasted control and NAFLD subjects (Figure 4F), suggesting that peripheral NEFA supply is not the sole factor responsible for promoting lipid catabolism in NAFLD.

An additional supply of substrate for hepatic β-oxidation may be derived from intrahepatic TG. This mechanism has been observed in patients with type 1 diabetes who develop hepatic steatosis during ketoacidosis: upon treatment with insulin, plasma ketone concentrations remain elevated due to the continued clearance of intrahepatic TG via ketogenesis-linked oxidative metabolism despite normalization of plasma NEFA concentrations (37). A role for intrahepatic lipolysis in humans is also consistent with data from our previous study of the effect of a 48-hour fast on hepatic TG content (20). Previously unpublished analysis of that data with respect to basal and fasted liver TG content (Supplemental Figure 5) demonstrates that fasting leads to a reduction in hepatic TG concentrations in individuals with higher basal liver fat, consistent with lipolytic release. Even larger amounts of intrahepatic lipid can be mobilized after only 2 weeks of weight loss (12). Thus, the pool of hepatic TG is quite labile, prone to lipolytic release, and available to support hepatic oxidative metabolism in the setting of fasting.

While glucagon and insulin signaling also regulate hepatic β-oxidation and ketogenesis directly, the effect of insulin resistance may either increase or decrease the function of these pathways. Some of the metabolic effects of insulin are retained during hepatic insulin resistance. Specifically, insulin continues to activate lipogenesis (38), which inhibits mitochondrial NEFA transport and β-oxidation (39). The nuanced alterations in cell signaling that give rise to elevated lipogenesis during insulin resistance can also suppress ketogenic flux by activating mTOR complex 1 (mTORC1) or activate TCA cycle flux by promoting FOXO targets (40). Indeed, the glucagon/insulin ratio had a complex relationship with hepatic β-oxidation ($r_S = 0.367$, $P = 0.030$) that included a positive correlation with ketogenesis ($r_S = 0.445$, $P = 0.006$) but a negative correlation with TCA cycle activity ($r_S = –0.584$, $P < 0.001$). These relationships are consistent with prior work with fed and fasted rodent livers (25), and indicate that an attenuated glucagon/insulin ratio contributes to the dysregulation of hepatic fat catabolism in NAFLD. However, the precise molecular mechanisms involved remain to be determined.

Elevated gluconeogenesis during insulin resistance and NAFLD is dependent on β-oxidation and the partitioning of acetyl-CoA between ketogenesis and the TCA cycle (41). In fact, insulin's direct inhibition of hepatic glucose production (42) is complemented by its suppression of plasma NEFAs, which indirectly inhibits gluconeogenic capacity (43). The stimulation of hepatic gluconeogenesis by β-oxidation is complex and mediated by its downstream effects, including ATP supply, energy charge, redox, and allosteric effectors such as citrate and acetyl-CoA. Notably, acetyl-CoA is an essential allosteric activator of pyruvate carboxylase (44), the predominant anaplerotic pathway that provides precursors for gluconeogenesis.

It was recently reemphasized that a rise in hepatic acetyl-CoA causes increased gluconeogenesis during insulin resistance (45). Since it is impractical and unsafe to examine acetyl-CoA directly in human liver tissue, we applied a recently reported noninvasive assay of liver acetyl-CoA based on in vivo ketone turnover (29). This assay indicated lower acetyl-CoA content in NAFLD subjects (Figure 3B), despite increased pyruvate carboxylase activation (Figure 2, B and C). In fact, neither ketogenesis nor estimated β-oxidation as indicators of hepatic acetyl-CoA content significantly correlated with rates of gluconeogenesis within the study population (Supplemental Figure 2B and Supplemental 4A). Hence, either ketone turnover as a marker of hepatic acetyl-CoA content (29) or acetyl-CoA as the principal mechanism of excess gluconeogenesis during insulin resistance (45) must be incorrect. It is possible that the dynamics of acetyl-CoA metabolism in human liver, in contrast to rodent liver (29), render its rate of production an inaccurate predictor of concentration and allosteric availability. However, it has also been frequently noted that a conceptual limitation of this mechanism is that the mitochondrial acetyl-CoA concentration is always much higher than required for allosteric activation of pyruvate carboxylase (46–51), especially in human liver (52, 53). Nevertheless, if elevated gluconeogenesis during NAFLD is impacted by altered β-oxidation, the mechanism may be related to *how* acetyl-CoA is metabolized rather than its rate of production.

Acetyl-CoA metabolism has important implications for cellular energy state, which is another mechanism by which β-oxidation can impinge on gluconeogenesis (54). Indeed, elevated gluconeogenesis was associated with increased oxidation of acetyl-CoA in the TCA cycle, which generates ≈3-fold more ATP than when β-oxidation is coupled to ketogenesis. Flux estimates of hepatic $\dot{V}O_2$ correlated closely with gluconeogenesis, consistent with respiration and ATP supply being important regulatory factors (54, 55). The shift to oxidation in the TCA cycle is essential because gluconeogenesis requires a high proportion of hepatic ATP production (56). In the absence of increased β-oxidation, this shift is predicated on a concomitant reduction in ketogenesis, as was observed here. Indeed, the simple elevation of gluconeogenic substrates is sufficient to stimulate the TCA cycle at the expense of ketogenesis (30). Specifically, pyruvate concentrations, which were elevated by ≈17% in NAFLD subjects, directly increase pyruvate carboxylase flux (51), elevate TCA function, and reduce the conversion of acetyl-CoA to ketones (30). It remains unclear whether elevated gluconeogenesis stimulates the TCA cycle and respiration, or vice versa, but increased respiration appears to precede the development of NASH in humans (18).

Decreased plasma concentrations of BHB under normally ketogenic conditions may be a general feature of NAFLD and NASH (27, 28) that plays an etiological role in the disease. Inhibition of ketogenesis in a rodent model shows striking similarities to human NAFLD and NASH, including increased gluconeogenesis, partitioning of acetyl-CoA to oxidation in the TCA cycle, and susceptibility to inflammation and liver injury (23, 24). The lower BHB (but not AcAc) production and impaired interconversion of BHB and AcAc observed in NAFLD subjects (Figure 3, D–F) might suggest a specific defect at the BHB dehydrogenase step of ketone metabolism (57). This enzyme requires a unique phospholipid interface with the inner mitochondrial membrane to function (58), which is disrupted by loss of insulin action (59). The loss of ketone production is particularly relevant to the inflammation that develops in NASH (2) because BHB inhibits inflammasome-mediated cytokines through signaling mechanisms (60) and AcAc oxidation by liver macrophages prevents the activation of fibrosis (61). Thus, ketosis may represent a reasonably tractable intervention against NAFLD. Fasting for 24 hours alone improves systemic inflammation in humans (62), and intermittent fasting (≈18–24 hours) followed by periods of normal feeding may have beneficial effects on insulin action (63). Even NAFLD subjects studied here following a 24-hour fast had increased ketogenesis and reduced TCA cycle activity compared with similar subjects studied in the postabsorptive state (7). Not surprisingly, ketogenic diets have an analogous effect in obese subjects (21), with the added benefit of rapidly reducing hepatic steatosis (64). It is notable that recent pharmacological targets, such as sodium glucose cotransporter 2 (SGLT2) inhibitors (65) and acetyl-CoA carboxylase 1/2 (ACC1/2) inhibitors (66) also activate ketogenesis. While it is clear that the ketogenic response is impaired in NAFLD, more investigations are required in order to understand whether this is a primary defect and whether interventions that enhance ketogenesis have long-term beneficial effects.

In conclusion, NAFLD subjects have disruptions in lipid catabolism characterized by altered hepatic acetyl-CoA partitioning between ketogenesis and the TCA cycle. When ketosis was induced by a 24-hour fast, ketogenesis was impaired and acetyl-CoA oxidation in the TCA cycle was concomitantly increased in those with fatty liver. The factors that contribute to the diminished response to fasting may be related to abnormal hormone signaling, a persistently low glucagon/insulin ratio, and related effects on circulating NEFAs and pyruvate. Elevated gluconeogenesis in NAFLD subjects cannot be explained by hepatic acetyl-CoA production determined

by ketone turnover or estimated β-oxidation but was positively associated with flux estimates of anaplerosis, TCA cycle activity, and respiration. It is unclear whether elevated oxidative metabolism stimulates gluconeogenesis or vice versa. In either case, the data suggest that activation of ketogenesis is a potential therapeutic recourse that may increase lipid disposal, reduce oxidative metabolism, and improve glucose homeostasis.

Methods

Participants. Forty nondiabetic individuals with and without a history of NAFLD were recruited for study at the University of Texas Southwestern (UTSW) Medical Center. Subjects consuming alcohol in excess (>30 g/d in men, >20 g/d in women), with a BMI >35 kg/m^2, with concurrent liver disease (other than NAFLD), or taking medications associated with hepatic steatosis were excluded from study. After hepatic TG content was determined by proton magnetic resonance spectroscopy (^{1}H-MRS), subjects were categorized into NAFLD (n = 23; range: 5%–52%) or control (n = 17; range: 0%–4%) groups based on a 5% cutoff value.

Design. The study schema is presented in Supplemental Figure 6. One week prior to isotope studies, all subjects underwent dual-energy X-ray absorptiometry (DEXA) to assess body fat distribution and lean mass, ^{1}H-MRS to determine hepatic TG content, and H-E clamp to measure insulin sensitivity. Subjects then maintained an ad libitum diet for 4 days, keeping a record of food intake to allow individual daily caloric intake to be determined. Subjects were then placed on a 3-day standard meal plan consisting of 50% carbohydrate, 35% fat, and 15% protein with a daily caloric intake reflective of their ad libitum diet. Frozen meals were provided to subjects for home consumption and prepared by the UTSW Clinical and Translational Research Center (CTRC) kitchen under the direction of a dietitian. The final standard meal occurred at 12:00 the day prior to isotopic studies, marking the beginning of a 24-hour fast. Subjects presented to the Advanced Imaging Research Center (AIRC) at 08:00 the following day to undergo the isotope studies to assess in vivo hepatic metabolism. Indirect calorimetry was performed prior to the H-E clamp as well as the isotope study (Vmax Encore, CareFusion).

H-E clamp. After an overnight fast (last meal at 18:30), subjects presented to the AIRC to undergo H-E clamp. Two intravenous catheters were placed — one was positioned in the antecubital fossa for infusion of insulin and 20% dextrose, and the other was placed retrograde in the dorsal contralateral hand to obtain blood samples. The hand with the retrograde catheter was placed in a hot box and maintained at 70°C during the procedure to arterialize the venous blood samples. Blood was drawn 20 and 10 minutes prior to the H-E clamp for chemistries as well as baseline glucose measurement. At t = 0 minutes, a 2-hour primed continuous infusion of human insulin was initiated at a rate of 80 mU/m^2 via a syringe pump (Harvard Apparatus). A variable infusion of 20% dextrose was initiated at t = +4 minutes to maintain euglycemia via an Alaris pump (BD). Arterialized blood samples were drawn every 5 minutes during the clamp to monitor plasma glucose concentrations (YSI Inc.). Blood was also obtained at t = +100 minutes and +110 minutes for chemistries. At the end of the infusion period, urine was collected, volume determined, and glucose concentration measured. The H-E clamp could not be completed in 1 control and 3 NAFLD subjects.

DEXA. Fat mass, fat-free mass, and bone mineral mass in the total body, trunk, lower body, and upper extremities were measured using DEXA scanning as previously described (67).

Hepatic TG content. Measurement of hepatic TG was done by ^{1}H-MRS using a 3.0 Tesla Achieva whole-body MR system (Philips Medical Systems). For single-voxel-localized data acquisition, a 2 × 2 × 2 cm^3 volume of interest was positioned in the right hepatic lobe, avoiding major blood vessels, intrahepatic bile ducts, and the lateral margins of liver. After the system was tuned and shimmed, spectra were collected using a combination of whole-body and SENSE torso coils for radiofrequency transmission and reception. The stimulated echo acquisition mode (STEAM) sequence was applied without suppression of water signal. Proton-MR spectra were acquired with interpulse delay Tr = 1.6 seconds, spin echo time Te = 14 ms, mixing time Tm = 18 ms, 16 acquisitions, and 2048 data points over a 1,500-Hz spectral width. The levels of hepatic TG were calculated from the area of methylene resonance (1.4 ppm) with respect to that of water resonance (4.8 ppm) as described previously (68).

Isotopes and other materials. Seventy-percent [^{2}H]water and 99% [U-$^{13}C_3$]propionate (sodium salt) were obtained from Cambridge Isotopes. Sterility- and pyrogen-tested [3,4-$^{13}C_2$]glucose (98%) was obtained from Omicron Biochemicals Inc. in sealed, stoppered vials. Sterility- and pyrogen-tested [3,4-$^{13}C_2$]ethylacetoacetate (98%) and [1,2-$^{13}C_2$]sodium BHB (98%) were obtained from Isotec in sealed, stoppered vials. Other common reagents were purchased from MilliporeSigma.

Infusate preparation. All preparation took place in a pharmacy-controlled ISO 7 cleanroom under a laminar flow hood using aseptic technique. Two hours prior to isotopic study, [3,4-$^{13}C_2$]ethylacetoacetate

was suspended in 6.6 ml of 0.5 M NaOH within its vial. The vial was then placed in an incubating shaker for 75 minutes at 40°C, followed by neutralization with 13.0 ml of 0.1 N HCl and buffering with 4.0 ml of 5% sodium bicarbonate. A 150-ml IntraVia bag (Baxter International) was used to deliver the tracers. The bag was first filled with 130 ml normal saline. The [3,4-$^{13}C_2$]glucose and [1,2-$^{13}C_2$]sodium BHB were each suspended in 10 ml saline within their respective vials. After mixing, the contents of these vials and the hydrolyzed [3,4-$^{13}C_2$]ethylacetoacetate vial were injected into the infusate bag through a 0.2-micron filter. The final volume of the isotope solution was calculated and written in the subject's chart.

Isotope infusion protocol. After a 3-day standard diet, subjects presented to the AIRC to undergo isotopic study. Between 22:00 and 12:00, subjects received 2 tracers orally: divided doses of 70% [^{2}H]water (5 g/kg body water, calculated as 60% of body weight in men and 50% of body weight in women) at 22:00, 02:00, and 06:00 and [U-$^{13}C_3$]propionate (≈400 mg) at 11:00, 11:30, and 12:00. Subjects were allowed to drink 0.5% [^{2}H]water ad libitum for the remainder of the study. The infusion began with a bolus of infusate calculated to deliver 2.25 mg/kg of [3,4-$^{13}C_2$]glucose at 12:00 (24 hours after last meal), followed by a 2-hour infusion (0.0225 mg [3,4-$^{13}C_2$]glucose/kg/min in conjunction with [3,4-$^{13}C_2$]AcAc and [1,2-$^{13}C_2$]BHB). At the end of the infusion period (14:00), a 50-cc blood draw was performed.

Measurement of glucose, AcAc, and BHB isotopomers. Plasma was extracted with perchloric acid, and glucose, AcAc, and BHB were purified as previously described (7, 69). Briefly, the supernatant was filtered by ion exchange chromatography, neutralized with LiOH, and then rapidly frozen. The frozen sample was then lyophilized until ≈500 μl remained using a speed-vacuum (Savant) and freeze-dryer (FTS systems). The final product was used for measurement of labeled ketone bodies using ^{13}C-NMR. The residual ketone sample was then desalted using ion exchange chromatography, followed by purification of plasma glucose and synthesis of 1,2-isopropylidene glucofuranose (monoacetone glucose [MAG]), as detailed previously (70–72). The MAG was then analyzed by ^{2}H- and ^{13}C-NMR to determine plasma glucose isotopomers. Samples were analyzed on a 14.1 T Varian Inova spectrometer (Varian Instruments) equipped with a 3-mm (MAG) or 5-mm (ketones) broadband probe tuned to 92 MHz for ^{2}H spectra or 150 MHz for ^{13}C spectra. Resonance areas were determined using ACD/Labs 12.0 (Advanced Chemistry Development Inc.). Ketone spectra were inadequate for analysis in 2 NAFLD subjects. Glucose spectra were inadequate for analysis in 2 control subjects.

Metabolic analysis. Deuterium signals from the H2 and H5 positions of MAG were used to determine the fraction of EGP originating from gluconeogenesis and glycogenolysis (fractional glucose production) (70, 73). Information from the H6s position allowed for the determination of the fraction of glucose produced from trioses originating from the TCA cycle as well as glycerol (73). Pathways intersecting the TCA cycle (gluconeogenesis, anaplerosis, and pyruvate cycling) were measured by ^{13}C-NMR analysis of glucose C2 isotopomers formed as a consequence of [U-$^{13}C_3$]propionate ingestion (49). EGP was measured by the dilution of [3,4-$^{13}C_2$]glucose as previously described (74). Absolute rates of gluconeogenesis and glycogenolysis were obtained by multiplying EGP by the fractional values determined by ^{2}H-NMR. Fluxes centered on the TCA cycle were calculated by indexing the relative fluxes obtained by ^{13}C-NMR to the absolute rate of production of glucose from trioses originating from the TCA cycle (75). Ketone turnover and rates of appearance, interconversion, and disappearance for both AcAc and BHB were calculated using a 2-pool model of exchangeable AcAc and BHB (69, 76–78). The combined metabolic flux data were used to estimate hepatic β-oxidation and oxygen consumption, as previously described (21, 79).

Metabolite and hormone measurements. Blood was collected in nonheparinized, EDTA-containing tubes and immediately centrifuged to isolate plasma. Samples were frozen and maintained at –80°C, after which they were thawed once and analyzed. ELISA kits were used to measure plasma concentrations of insulin, glucagon (Millipore), and free fatty acids (Wako Chemicals USA). Plasma ketone concentrations were determined using a commercial kit (Wako Chemicals USA). Other chemistries were performed by an outside laboratory (Quest Diagnostics).

To measure organic acids in blood, 50 μl plasma was mixed with 0.8% sulfosalicylic acid and 5 M hydroxylamine-HCl solution, and centrifuged (21,000 *g*, 10 minutes, 4°C). The supernatant was neutralized with 2 M KOH to pH 6–7 and then incubated at 65°C for 60 minutes. The reaction mixture was acidified using 2 M HCl (pH 1–2), saturated with sodium chloride, and extracted with ethyl acetate. The dried extract was dissolved with acetonitrile and MTBSTFA as silylation reagent and incubated at 60°C for 60 minutes. The derivatives were analyzed in both scan and SIM modes by using an Agilent 7890A gas chromatograph interfaced to an Agilent 5975C mass-selective detector (70 eV, electron ionization source). An HP-5ms GC column (30 m × 0.25 mm I.D., 0.25 μm film thickness) was used for all analysis (80).

Statistics. Statistical analyses were performed using SigmaPlot 13.0 (Systat Software Inc.). Differences between groups were evaluated using the 2-tailed Student's *t* test for paired and unpaired data and ANOVA as appropriate. Proportions were analyzed by χ^2 and Fisher's exact test. Strength and significance of correlations were determined by Spearman's rank-order. Unless otherwise indicated, values are presented as mean with SEM. Statistical significance was taken at $P < 0.05$.

Study approval. This study was conducted according to Declaration of Helsinki principles and approved by the Institutional Review Board of UTSW. Each participant provided written informed consent before participation.

Author contributions

JDB and SCB were responsible for conceptualization, data curation, formal analysis, funding acquisition, investigation, methodology, project administration, resources, supervision, visualization, writing — original draft, and writing — review and editing. JAF and SD were equally responsible for data curation, formal analysis, investigation, methodology, writing — original draft, and writing — review and editing. SS and XF were responsible for data curation, formal analysis, and investigation.

Acknowledgments

We would like to thank Jeannie Baxter, Carol Parcel, Lucy Christie, and Kelley Derner (AIRC nursing staff) for assistance with coordination and conduct of the study. We also greatly appreciate the thoughtful discussions and review of the manuscript by Jay D. Horton. This research was supported by the Robert A. Welch Foundation I-1804 (SCB and SD), NIH R01DK087977 (JDB), NIH PL1DK081183 (JDB), NIH R01DK078184 (SCB), NIH F32DK107124 (JAF), and NIH P41EB015908 (SCB and SD).

Address correspondence to: Jeffrey D. Browning, Department of Clinical Nutrition, 6011 Harry Hines Blvd, Dallas, Texas 75390, USA. Phone: 214.648.5987; Email: jeffrey.browning@utsouthwestern.edu. Or to: Shawn C. Burgess, Center for Human Nutrition, 5323 Harry Hines Blvd, Dallas, Texas 75390, USA. Phone: 214.645.2728; Email: shawn.burgess@utsouthwestern.edu.

1. Ludwig J, Viggiano TR, McGill DB, Oh BJ. Nonalcoholic steatohepatitis: Mayo Clinic experiences with a hitherto unnamed disease. *Mayo Clin Proc*. 1980;55(7):434–438.
2. Browning JD, Horton JD. Molecular mediators of hepatic steatosis and liver injury. *J Clin Invest*. 2004;114(2):1–4.
3. Browning JD, et al. Prevalence of hepatic steatosis in an urban population in the United States: impact of ethnicity. *Hepatology*. 2004;40(6):1387–1395.
4. US Census Bureau, Population Division. Annual Estimates of the Residential Population: April 1, 2010 to July 1, 2017. American FactFinder website. https://factfinder.census.gov/faces/tableservices/jsf/pages/productview.xhtml?src=bkmk. Accessed January 24, 2019.
5. Donnelly KL, Smith CI, Schwarzenberg SJ, Jessurun J, Boldt MD, Parks EJ. Sources of fatty acids stored in liver and secreted via lipoproteins in patients with nonalcoholic fatty liver disease. *J Clin Invest*. 2005;115(5):1343–1351.
6. Lambert JE, Ramos-Roman MA, Browning JD, Parks EJ. Increased de novo lipogenesis is a distinct characteristic of individuals with nonalcoholic fatty liver disease. *Gastroenterology*. 2014;146(3):726–735.
7. Sunny NE, Parks EJ, Browning JD, Burgess SC. Excessive hepatic mitochondrial TCA cycle and gluconeogenesis in humans with nonalcoholic fatty liver disease. *Cell Metab*. 2011;14(6):804–810.
8. Balasse EO. Kinetics of ketone body metabolism in fasting humans. *Metabolism*. 1979;28(1):41–50.
9. Wolever TM, Bentum-Williams A, Jenkins DJ. Physiological modulation of plasma free fatty acid concentrations by diet. Metabolic implications in nondiabetic subjects. *Diabetes Care*. 1995;18(7):962–970.
10. Gershuni VM, Yan SL, Medici V. Nutritional ketosis for weight management and reversal of metabolic syndrome. *Curr Nutr Rep*. 2018;7(3):97–106.
11. Sutton EF, Beyl R, Early KS, Cefalu WT, Ravussin E, Peterson CM. Early time-restricted feeding improves insulin sensitivity, blood pressure, and oxidative stress even without weight loss in men with prediabetes. *Cell Metab*. 2018;27(6):1212–1221.e3.
12. Browning JD, Baker JA, Rogers T, Davis J, Satapati S, Burgess SC. Short-term weight loss and hepatic triglyceride reduction: evidence of a metabolic advantage with dietary carbohydrate restriction. *Am J Clin Nutr*. 2011;93(5):1048–1052.
13. Reddy JK, Mannaerts GP. Peroxisomal lipid metabolism. *Annu Rev Nutr*. 1994;114:343–370.
14. Felig P, Wahren J, Hendler R, Brundin T. Splanchnic glucose and amino acid metabolism in obesity. *J Clin Invest*. 1974;53(2):582–590.
15. Brundin T, Thorne A, Wahren J. Heat leakage across the abdominal wall and meal-induced thermogenesis in normal-weight and obese subjects. *Metabolism*. 1992;41(1):49–55.
16. Iozzo P, et al. Fatty acid metabolism in the liver, measured by positron emission tomography, is increased in obese individuals. *Gastroenterology*. 2010;139(3):846–856.
17. Hyotylainen T, et al. Genome-scale study reveals reduced metabolic adaptability in patients with non-alcoholic fatty liver disease. *Nat Commun*. 2016;7:8994.

18. Koliaki C, et al. Adaptation of hepatic mitochondrial function in humans with non-alcoholic fatty liver is lost in steatohepatitis. *Cell Metab*. 2015;21(5):739–746.
19. Morris EM, Rector RS, Thyfault JP, Ibdah JA. Mitochondria and redox signaling in steatohepatitis. *Antioxid Redox Signal*. 2011;15(2):485–504.
20. Browning JD, Baxter J, Satapati S, Burgess SC. The effect of short-term fasting on liver and skeletal muscle lipid, glucose, and energy metabolism in healthy women and men. *J Lipid Res*. 2012;53(3):577–586.
21. Browning JD, et al. Alterations in hepatic glucose and energy metabolism as a result of calorie and carbohydrate restriction. *Hepatology*. 2008;48(5):1487–1496.
22. Satapati S, et al. Mitochondrial metabolism mediates oxidative stress and inflammation in fatty liver. *J Clin Invest*. 2015;125(12):4447–4462.
23. Cotter DG, et al. Ketogenesis prevents diet-induced fatty liver injury and hyperglycemia. *J Clin Invest*. 2014;124(12):5175–5190.
24. d'Avignon DA, et al. Hepatic ketogenic insufficiency reprograms hepatic glycogen metabolism and the lipidome. *JCI Insight*. 2018;3(12):e99762.
25. McGarry JD, Foster DW. The regulation of ketogenesis from octanoic acid. The role of the tricarboxylic acid cycle and fatty acid synthesis. *J Biol Chem*. 1971;246(4):1149–1159.
26. Satapati S, et al. Elevated TCA cycle function in the pathology of diet-induced hepatic insulin resistance and fatty liver. *J Lipid Res*. 2012;53(6):1080–1092.
27. Mannisto VT, et al. Ketone body production is differentially altered in steatosis and non-alcoholic steatohepatitis in obese humans. *Liver Int*. 2015;35(7):1853–1861.
28. Inokuchi T, Orita M, Imamura K, Takao T, Isogai S. Resistance to ketosis in moderately obese patients: influence of fatty liver. *Intern Med*. 1992;31(8):978–983.
29. Perry RJ, Peng L, Cline GW, Petersen KF, Shulman GI. A Non-invasive method to assess hepatic acetyl-CoA in vivo. *Cell Metab*. 2017;25(3):749–756.
30. Beatty CH, West ES. The effect of substances related to the tricarboxylic acid cycle upon ketosis. *J Biol Chem*. 1951;190(2):603–610.
31. Randle PJ. Regulatory interactions between lipids and carbohydrates: the glucose fatty acid cycle after 35 years. *Diabetes Metab Rev*. 1998;14(4):263–283.
32. McGarry JD, Foster DW. Regulation of ketogenesis and clinical aspects of the ketotic state. *Metabolism*. 1972;21(5):471–489.
33. Klein S, et al. Gastric bypass surgery improves metabolic and hepatic abnormalities associated with nonalcoholic fatty liver disease. *Gastroenterology*. 2006;130(6):1564–1572.
34. Fabbrini E, Mohammed BS, Magkos F, Korenblat KM, Patterson BW, Klein S. Alterations in adipose tissue and hepatic lipid kinetics in obese men and women with nonalcoholic fatty liver disease. *Gastroenterology*. 2008;134(2):424–431.
35. Wolfe RR, et al. Effect of short-term fasting on lipolytic responsiveness in normal and obese human subjects. *Am J Physiol*. 1987;252(2 pt 1):E189–EE96.
36. Buijs MM, et al. Blunted lipolytic response to fasting in abdominally obese women: evidence for involvement of hyposomatotropism. *Am J Clin Nutr*. 2003;77(3):544–550.
37. Van Harken DR, Dixon CW, Heimberg M. Hepatic lipid metabolism in experimental diabetes. V. The effect of concentration of oleate on metabolism of triglycerides and on ketogenesis. *J Biol Chem*. 1969;244(9):2278–2285.
38. Brown MS, Goldstein JL. Selective versus total insulin resistance: a pathogenic paradox. *Cell Metab*. 2008;7(2):95–96.
39. McGarry JD, Leatherman GF, Foster DW. Carnitine palmitoyltransferase I. The site of inhibition of hepatic fatty acid oxidation by malonyl-CoA. *J Biol Chem*. 1978;253(12):4128–4136.
40. Kucejova B, et al. Hepatic mTORC1 opposes impaired insulin action to control mitochondrial metabolism in obesity. *Cell Rep*. 2016;16(2):508–519.
41. Williamson JR, Wright PH, Malaisse WJ, Ashmore J. Control of gluconeogenesis by acetyl CoA in rats treated with glucagon and anti-insulin serum. *Biochem Biophys Res Commun*. 1966;24(5):765–770.
42. Cherrington AD. The role of hepatic insulin receptors in the regulation of glucose production. *J Clin Invest*. 2005;115(5):1136–1139.
43. Bergman RN, Iyer MS. Indirect regulation of endogenous glucose production by insulin: the single gateway hypothesis revisited. *Diabetes*. 2017;66(7):1742–1747.
44. Utter MF, Keech DB. Pyruvate carboxylase. I. Nature of the reaction. *J Biol Chem*. 1963;238:2603–2608.
45. Perry RJ, et al. Hepatic acetyl CoA links adipose tissue inflammation to hepatic insulin resistance and type 2 diabetes. *Cell*. 2015;160(4):745–758.
46. Scrutton MC. Pyruvate carboxylase. Studies of activator-independent catalysis and of the specificity of activation by acyl derivatives of coenzyme A for the enzyme from rat liver. *J Biol Chem*. 1974;249(22):7057–7067.
47. Williamson JR, Browning ET, Olson M. Interrelations between fatty acid oxidation and the control of gluconeogenesis in perfused rat liver. *Adv Enzyme Regul*. 1968;6:67–100.
48. Siess EA, Brocks DG, Wieland OH. Distribution of metabolites between the cytosolic and mitochondrial compartments of hepatocytes isolated from fed rats. *Hoppe Seylers Z Physiol Chem*. 1978;359(7):785–798.
49. Jones JG, Naidoo R, Sherry AD, Jeffrey FM, Cottam GL, Malloy CR. Measurement of gluconeogenesis and pyruvate recycling in the rat liver: a simple analysis of glucose and glutamate isotopomers during metabolism of [1,2,3-(13)C3]propionate. *FEBS Lett*. 1997;412(1):131–137.
50. Martin-Requero A, Corkey BE, Cerdan S, Walajtys-Rode E, Parrilla RL, Williamson JR. Interactions between alpha-ketoisovalerate metabolism and the pathways of gluconeogenesis and urea synthesis in isolated hepatocytes. *J Biol Chem*. 1983;258(6):3673–3681.
51. McClure WR, Lardy HA, Wagner M, Cleland WW. Rat liver pyruvate carboxylase. II. Kinetic studies of the forward reaction. *J Biol Chem*. 1971;246(11):3579–3583.
52. Jitrapakdee S, Walker ME, Wallace JC. Functional expression, purification, and characterization of recombinant human pyruvate carboxylase. *Biochem Biophys Res Commun*. 1999;266(2):512–517.
53. Scrutton MC, White MD. Prufication and properties of human liver pyruvate carboxylase. *Biochem Med*. 1974;9(3):217–292.
54. Quinlan PT, Halestrap AP. The mechanism of the hormonal activation of respiration in isolated hepatocytes and its importance

in the regulation of gluconeogenesis. *Biochem J*. 1986;236(3):789–800.
55. Henly DC, Berry MN. Effect of palmitate concentration on the relative contributions of the beta-oxidation pathway and citric acid cycle to total O2 consumption of isolated rat hepatocytes. *Biochim Biophys Acta*. 1993;1175(3):269–276.
56. Williamson JR, Jakob A, Scholz R. Energy cost of gluconeogenesis in rat liver. *Metabolism*. 1971;20(1):13–26.
57. Lehninger AL, Sudduth HC, Wise JB. D-beta-Hydroxybutyric dehydrogenase of mitochondria. *J Biol Chem*. 1960;235:2450–2455.
58. Latruffe N, Berrez JM, el Kebbaj MS. Lipid-protein interactions in biomembranes studied through the phospholipid specificity of D-beta-hydroxybutyrate dehydrogenase. *Biochimie*. 1986;68(3):481–491.
59. Vidal JC, McIntyre JO, Churchill P, Andrew JA, Pehuet M, Fleischer S. Influence of diabetes on rat liver mitochondria: decreased unsaturation of phospholipid and D-beta-hydroxybutyrate dehydrogenase activity. *Arch Biochem Biophys*. 1983;224(2):643–658.
60. Youm YH, et al. The ketone metabolite beta-hydroxybutyrate blocks NLRP3 inflammasome-mediated inflammatory disease. *Nat Med*. 2015;21(3):263–269.
61. Puchalska P, et al. Hepatocyte-macrophage acetoacetate shuttle protects against tissue fibrosis. *Cell Metab*. 2019;29(2):383–398.e7.
62. Traba J, et al. Fasting and refeeding differentially regulate NLRP3 inflammasome activation in human subjects. *J Clin Invest*. 2015;125(12):4592–4600.
63. Halberg N, et al. Effect of intermittent fasting and refeeding on insulin action in healthy men. *J Appl Physiol (1985)*. 2005;99(6):2128–2136.
64. Browning JD, Davis J, Saboorian MH, Burgess SC. A low-carbohydrate diet rapidly and dramatically reduces intrahepatic triglyceride content. *Hepatology*. 2006;44(2):487–488.
65. Taylor SI, Blau JE, Rother KI. SGLT2 inhibitors may predispose to ketoacidosis. *J Clin Endocrinol Metab*. 2015;100(8):2849–2852.
66. Kim CW, et al. Acetyl CoA carboxylase inhibition reduces hepatic steatosis but elevates plasma triglycerides in mice and humans: a bedside to bench investigation. *Cell Metab*. 2017;26(2):394–406.e6.
67. Vega GL, Adams-Huet B, Peshock R, Willett D, Shah B, Grundy SM. Influence of body fat content and distribution on variation in metabolic risk. *J Clin Endocrinol Metab*. 2006;91(11):4459–4466.
68. Szczepaniak LS, et al. Magnetic resonance spectroscopy to measure hepatic triglyceride content: prevalence of hepatic steatosis in the general population. *Am J Physiol Endocrinol Metab*. 2005;288(2):E462–E468.
69. Satapati S, et al. Partial resistance to peroxisome proliferator-activated receptor-alpha agonists in ZDF rats is associated with defective hepatic mitochondrial metabolism. *Diabetes*. 2008;57(8):2012–2021.
70. Landau BR, Wahren J, Chandramouli V, Schumann WC, Ekberg K, Kalhan SC. Use of $^{2}H_{2}O$ for estimating rates of gluconeogenesis. Application to the fasted state. *J Clin Invest*. 1995;95(1):172–178.
71. Burgess SC, et al. Analysis of gluconeogenic pathways in vivo by distribution of 2H in plasma glucose: comparison of nuclear magnetic resonance and mass spectrometry. *Anal Biochem*. 2003;318(2):321–324.
72. Burgess SC, et al. Noninvasive evaluation of liver metabolism by 2H and 13C NMR isotopomer analysis of human urine. *Anal Biochem*. 2003;312(2):228–234.
73. Jones JG, Solomon MA, Cole SM, Sherry AD, Malloy CR. An integrated (2)H and (13)C NMR study of gluconeogenesis and TCA cycle flux in humans. *Am J Physiol Endocrinol Metab*. 2001;281(4):E848–E856.
74. Jin ES, Jones JG, Burgess SC, Merritt ME, Sherry AD, Malloy CR. Comparison of [3,4-13C2]glucose to [6,6-2H2]glucose as a tracer for glucose turnover by nuclear magnetic resonance. *Magn Reson Med*. 2005;53(6):1479–1483.
75. Burgess SC, et al. Impaired tricarboxylic acid cycle activity in mouse livers lacking cytosolic phosphoenolpyruvate carboxykinase. *J Biol Chem*. 2004;279(47):48941–48949.
76. Miles JM, Schwenk WF, McClean KL, Haymond MW. A dual-isotope technique for determination of in vivo ketone body kinetics. *Am J Physiol*. 1986;251(2 pt 1):E185–E191.
77. Bougneres PF, Ferre P. Study of ketone body kinetics in children by a combined perfusion of 13C and 2H3 tracers. *Am J Physiol*. 1987;253(5 pt 1):E496–502.
78. Bailey JW, Haymond MW, Miles JM. Validation of two-pool model for in vivo ketone body kinetics. *Am J Physiol*. 1990;258(5 pt 1):E850–E855.
79. Satapati S, et al. Mitochondrial metabolism mediates oxidative stress and inflammation in fatty liver. *J Clin Invest*. 2015;125(12):4447–4462.
80. Des Rosiers C, Fernandez CA, David F, Brunengraber H. Reversibility of the mitochondrial isocitrate dehydrogenase reaction in the perfused rat liver. Evidence from isotopomer analysis of citric acid cycle intermediates. *J Biol Chem*. 1994;269(44):27179–27182.